

## SUPPLEMENTARY TABLES

SMA	styrene:maleic acid	Mw (g/mol)	Mn (g/mol)	Source
SMA2000	2:1	7500	3000	Cray Valley
SMA3000	3:1	9500	3800	Cray Valley
Xiran SZ25010	3:1	10000	4000	Polyscope*
Xiran SZ30010	2.3:1	6500	2500	Polyscope*
Xiran SZ40005	1.2:1	5000	2000	Polyscope*

**Table S1. Characteristics of commercially-available SMA copolymers – Related to Figure 2**

The SMA 2000 copolymer is produced by Cray Valley and the Xiran SMA-copolymers are manufactured by Polyscope. \*The SMA manufactured by Polyscope is now sold by their subsidiary Polyscience.

Variant	Expression with BCN, %	Expression without BCN, %	Amber suppression efficiency, %	Labeling efficiency, %
F12	0	0	0	nd
V17	59	0	59	86 ±2
L31	21	0	21	95 ±3
L33	0	0	0	nd
L49	14	0	14	~25
E51	0	0	0	nd
K69	1	2	-1	~10
R66	0	0	0	nd
E71	2	4	-2	nd
L72	12	1	11	10
A81	0	0	0	nd
I85	42	2	40	88 ±2
F98	2	1	1	nd
K123	8	0	8	~10
E124	1	2	-1	nd
K130	2	5	-3	nd
I147	11	10	1	nd
L166	19	1	18	95 ±1
L177	51	16	35	80 ±1

**Table S2. Summary of the expression yields of PglC variants, normalized to the expression of WT PglC, in the presence or absence of BCN – Related to Figure 3**

The labeling efficiency is also reported (labeling efficiencies above 50 % are reported as mean ± SEM, n = 3; replicates were performed on distinct CEF aliquots). Residues in the hydrophobic domain are shown in red and residues in the soluble cytosolic domain are shown in green.

Variant	Suppression with BCN, %	Suppression without BCN, %	Amber suppression efficiency, %	Labeling efficiency, %
L47	0	0	0	nd
Y72	1	0	1	nd
W102	80	0	80	94
V132	0	0	0	nd
N134	19	0	19	104
S135	0	0	0	nd
F143	1	2	-1	nd
H145	28	0	28	89
T226	67	9	58	36
K321	61	8	63	51

**Table S3. Summary of the expression yields of PglA variants, normalized by the expression of WT PglA, in the presence or absence of BCN – Related to Figure 3**

The labeling efficiency is also reported. Residues in the hydrophobic domain are shown in red and residues in the soluble cytosolic domain are shown in green.

## SUPPLEMENTARY FIGURES

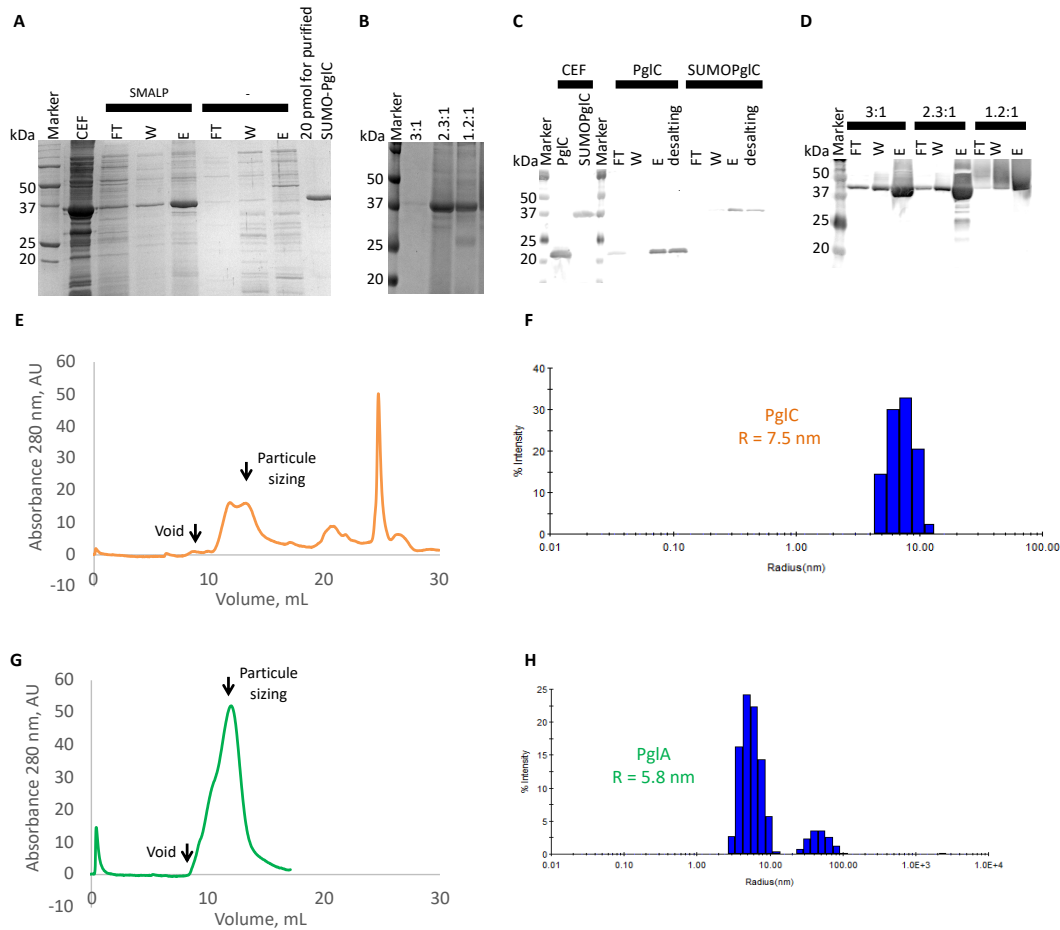


**Figure S1. Solubilization of SUMO-PglC, PglC and PglA using the styrene-maleic acid polymer – Related to Figure 2**

(A) SDS-PAGE gels analysis of the cell envelope fraction (CEF) as well as of the flow-through (FT), wash (W) and elution (E) fractions from the Ni<sup>2+</sup>-affinity purification of SUMO-PglC in the presence of SMA 2000. A sample was treated under the same conditions without addition of the SMA as a negative control. In the absence of SMA, the protein is not significantly present in any of the fraction, demonstrating that the polymer is needed to solubilize SUMO-PglC.

(B) SDS-PAGE gel analysis of the elution fractions after SMA-solubilization of SUMO-PglC. This construct can be efficiently purified in the presence of the 2.3:1 and 1.2:1 SMA copolymers.

(C) Anti-His western blot analysis of the expression and purification of PglC and SUMO-PglC using the 2.3:1 SMA. CEF: cell envelope fraction; FT: the flow-through; W: wash; E: elution step.

(D) Anti-His western blot analysis of the expression and purification of PglA using three different SMA copolymers. CEF: cell envelope fraction; FT: the flow-through; W: wash; E: elution step.

(E) Size-exclusion analysis of PglC in 2.3:1 SMA after Ni<sup>2+</sup>-affinity purification (absorbance followed at 280 nm).

(F) Size of the PglC SMA as evaluated by dynamic light scattering. PglC in SMA has a hydrodynamic diameter of 7.4 nm (25 % polydispersity).

(G) Size-exclusion analysis of PglA in 2.3:1 SMA after Ni<sup>2+</sup>-affinity purification (absorbance monitored at 280 nm).

(H) Size of the PglA SMA as evaluated by dynamic light scattering. PglA in SMA has a hydrodynamic diameter of 5.8 nm (31 % polydispersity).

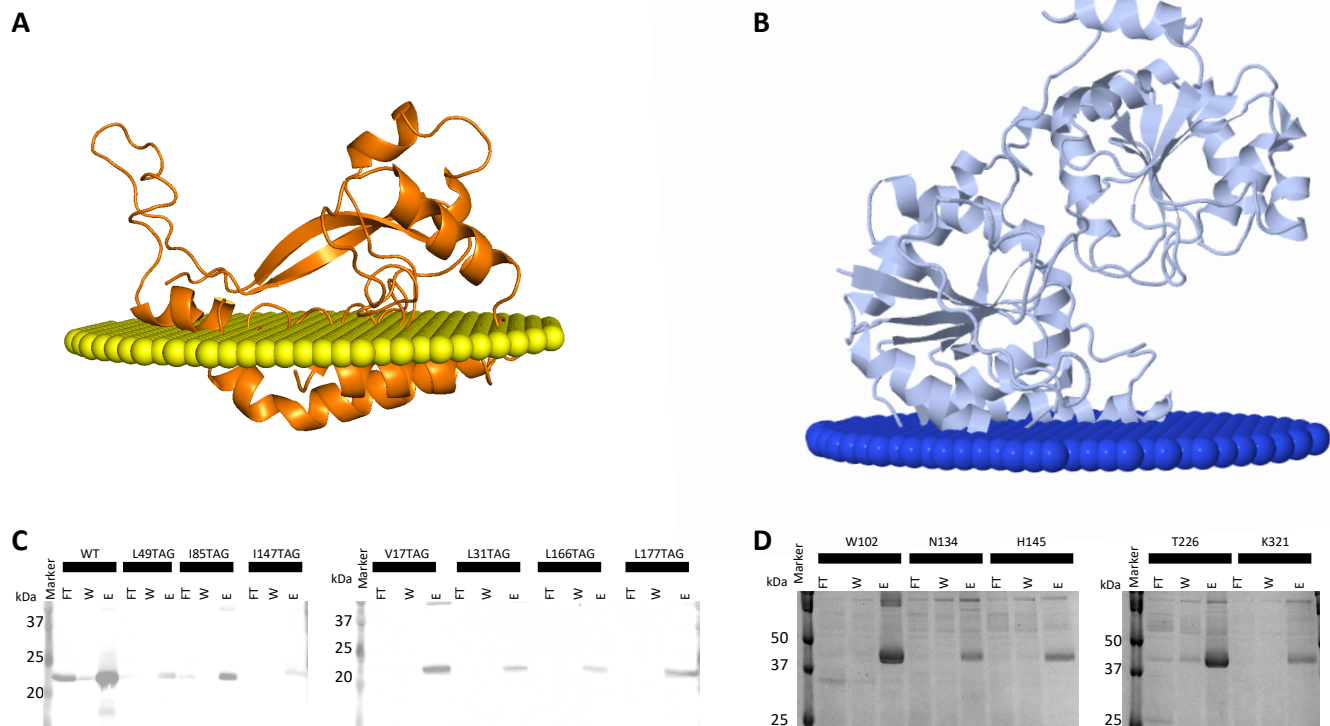


**Figure S2. Non-canonical amino acid mutagenesis applied to PglC and PglA – Related to Figures 3 and 4**

(A) The structure of PglC from *C. jejuni* was predicted with the online server iTasser using the PglC crystal structure (PDB: 5W7L) from *C. concisus* as template (Ray et al., 2018; Roy et al., 2010; Yang et al., 2015; Zhang, 2008) and the position of PglC with respect to the membrane plane was determined using the server “Orientations of Proteins in Membranes” (Lomize et al., 2012).

(B) The structure of PglA from *C. jejuni* was predicted with the online server iTasser using the structure of the glycosyl transferases WbnH (PDB: 4XYW) from *E. coli* as the template (Martinez-Fleites et al., 2006; Roy et al., 2010; Yang et al., 2015; Zhang, 2008) and the position of PglA with respect to the membrane plane determined using the server “Orientations of Proteins in Membranes” (Lomize et al., 2012).

(C) Efficiency of the purification of PglC variants in SMA-lipoparticles. Anti-His western blot analysis of the Ni<sup>2+</sup>-NTA purification of PglC V17, L31, L49, I85, I147, L166 and L177TAG variants after solubilization using the 2.3:1 SMA. FT: flow-through fraction; W: wash step; E: elution step.

(D) Efficiency of the purification of PglA variants in SMA-lipoparticles. SDS-PAGE analysis of the Ni<sup>2+</sup>-NTA purification of PglA W102, N134 and H145TAG variants after solubilization using the 2.3:1 SMA (Coomassie staining). FT: flow-through fraction; W: wash step; E: elution step.

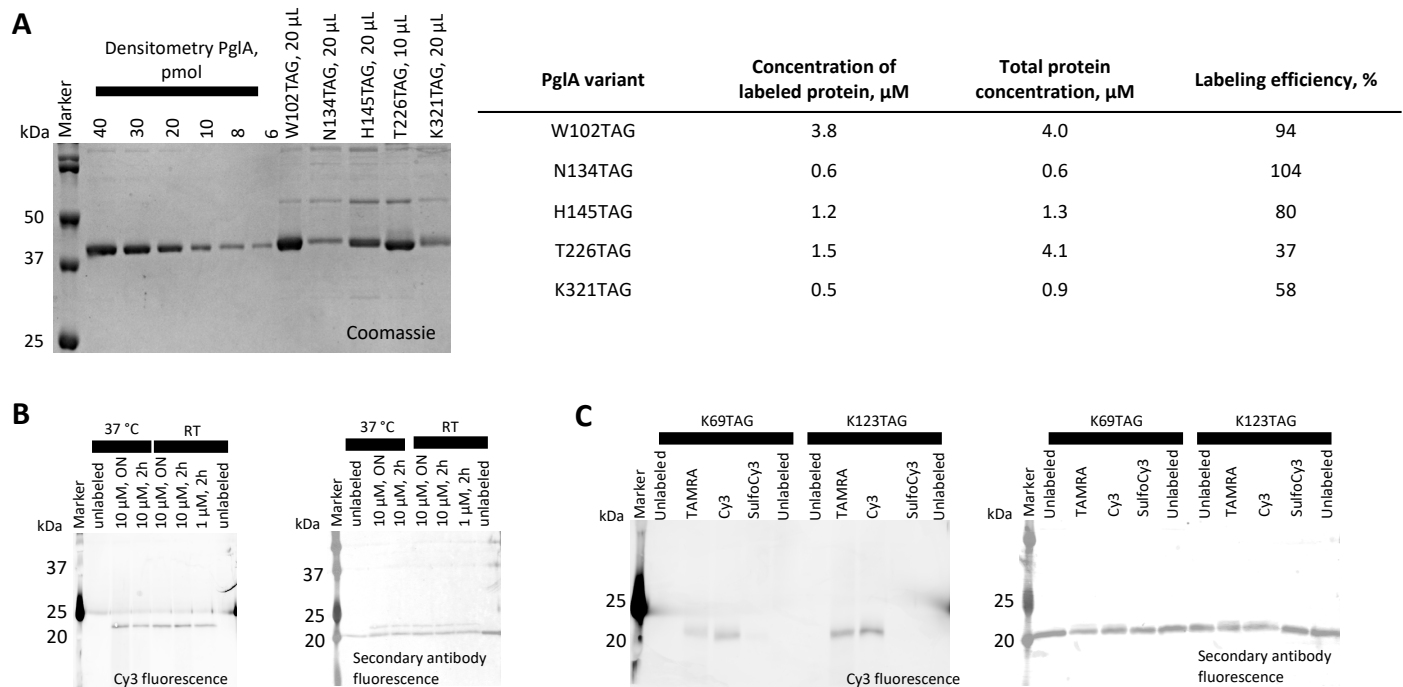


**Figure S3. Biorthogonal labeling of membrane proteins in SMALP – Related to Figure 4**

(A). Determination of the labeling efficiency of PglA. For PglA, labeling efficiency could not be evaluated by gel shift assay due to the higher molecular weight of PglA (37 kDa; as compared to PglC, 24 kDa). As a consequence, labeling efficiency was determined by independently measuring the total protein concentration (by densitometry; SDS-PAGE, left) and the concentration of the labeled protein (by absorption using the Cy3 chromophore). The total concentration of each PglA variant was determined by gel densitometry using WT PglA purified in the DIBMA copolymer as a standard. The DIBMA copolymer (BASF) is an analogue of SMA that does not absorb at 280 nm (Oluwole et al., 2017). The concentration of labeled protein was determined by measuring the absorbance at 550 nm of the SMA-solubilized and labeled PglA variant ( $\epsilon(\text{Cy3}) = 150,000 \text{ mol}\cdot\text{L}^{-1}\cdot\text{cm}^{-1}$ ). The labeling efficiency was calculated as the ratio between the concentration of labeled protein over the total protein concentration and reported in the table (right).

(B) Screening experimental conditions for an improved labeling of PglC variant: the labeling efficiency of PglC does not increase with increased time, concentration or temperature. PglC<sup>L49TAG</sup> was reacted with Cy3-tetrazine (1 to 10  $\mu\text{M}$ , 2 h to overnight (ON), room temperature (RT) or at 37 °C) and purified using a spin desalting column. Left: imaging of the western blot membrane showing the Cy3 fluorescence. Right: Anti-His western blot of the same SDS-PAGE.

(C) Screening experimental conditions for an improved labeling of PglC variant: Cy3-tetrazine is more reactive than sulfoCy3-methyltetrazine and comparable to TAMRA-tetrazine (Chen and Wu, 2016). PglC<sup>K69TAG</sup> and PglC<sup>K123TAG</sup> were reacted with TAMRA-tetrazine, Cy3-tetrazine or sulfoCy3-methyltetrazine (1  $\mu\text{M}$ , 2 h, room temperature or) and purified using a spin desalting column. Left: imaging of the western blot membrane showing the fluorescence from TAMRA, Cy3 and sulfo-Cy3 dyes. Right: Anti-His western blot of the same SDS-PAGE.

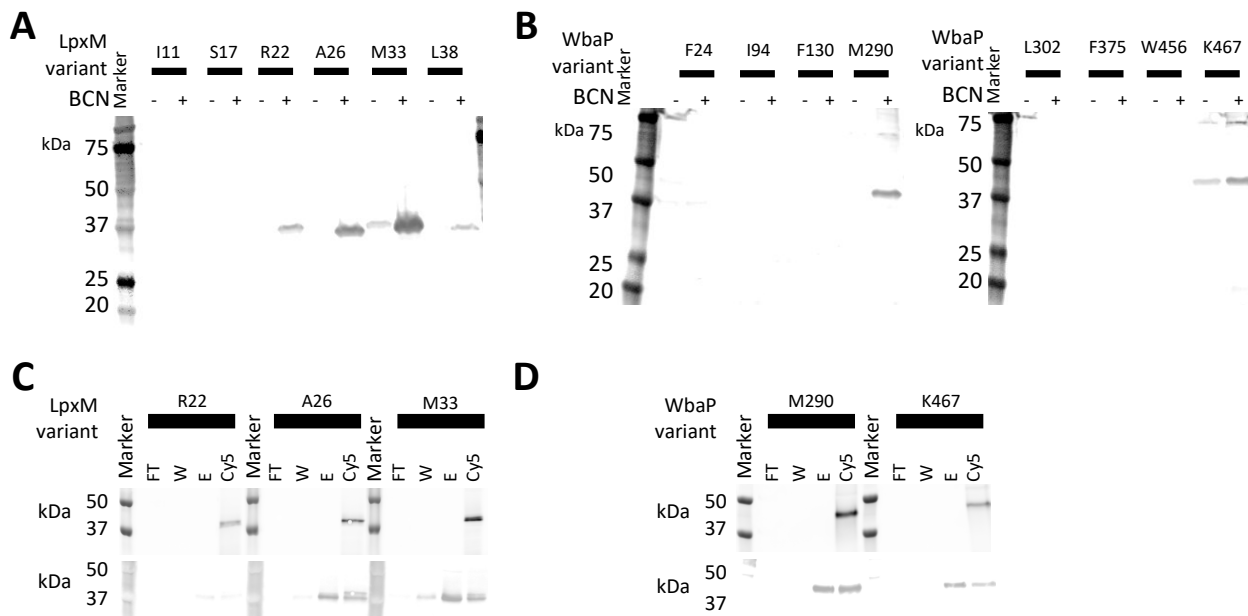


**Figure S4. Incorporation on the BCN non-canonical amino acid into LpxM (*E. coli*) and WbaP (*S. enterica*) followed by labeling with a tetrazine-linked Cy5 fluorophore derivative – Related to Figure 4**

(A) Anti-His western blot after expression of six LpxM variants. Residues R22, A26, M33 and L38 can be efficiently substituted by BCN.

(B) Anti-His western blot after expression of six WbaP variants. Residues M290 and M467 can be efficiently substituted by BCN.

(C) Imaging of a western blot membrane showing Cy5 fluorescence of three distinct LpxM variants (top). Anti-His western blot of the same SDS-PAGE (bottom). LpxM variants are 38 kDa, labeled LpxM-Cy5 variants are 39 kDa. FT: Flow-Through; W: Wash; E: Elution; Cy5: after labeling with Cy5-tetrazine.

(D) Imaging of a western blot membrane showing Cy5 fluorescence of three distinct WbaP variants (top). Anti-His western blot of the same SDS-PAGE (bottom). WbaP variants are 58 kDa, labeled WbaP-Cy5 variants are 59 kDa. FT: Flow-Through; W: Wash; E: Elution; Cy5: after labeling with Cy5-tetrazine.

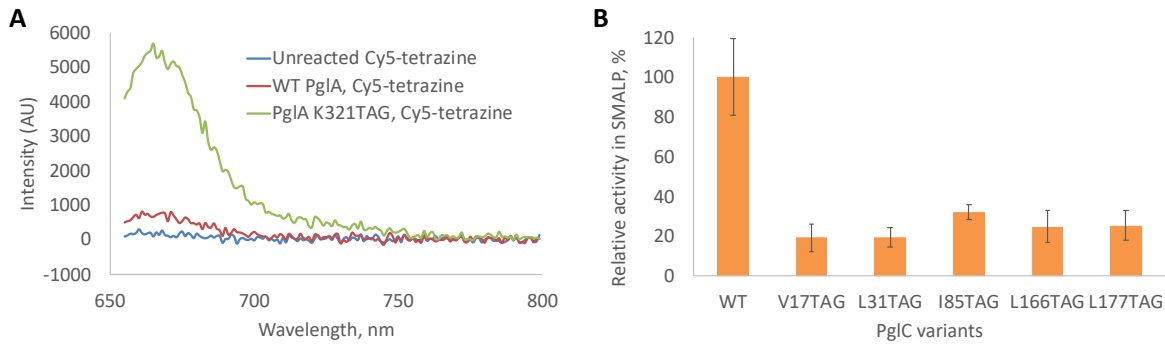


**Figure S5. Validation of the samples used for the determination of the loading of PglC and PglA SMA-lipoparticles – Related to Figure 5**

(A) Efficiency of the separation of unreacted tetrazine dyes using a desalting spin column. The eluted fractions of PglA WT and K321TAG variant were reacted with Cy5-tetrazine (Jena Biosciences). The solution was gently rocked at room temperature for 1 hour. As a positive control, we also incubated Cy5-tetrazine in buffer. The SMALPed protein was purified from the free dye using a spin desalting column, 7 kDa molecular weight cut-off (Thermofisher). The fluorescence of the flow-through was measured by fluorescence (excitation at 648 nm, emission recorded between 655 and 800, excitation and emission slits, 2 nm).

(B) Activity of Cy5-labeled PglC variants in SMALP. Activity was quantified using the UMP-Glo assay and normalized to PglC WT in SMALP. Data are represented as mean  $\pm$  SEM, n = 3; replicates were performed on distinct aliquots taken from a common protein purification using SMA for solubilization.